MCB
Journals.ASM.org

Stabilization of ATF5 by TAK1–Nemo-Like Kinase Critically Regulates the Interleukin-1β-Stimulated C/EBP Signaling Pathway

Ze-Yan Zhang,[a] Shang-Ze Li,[a] Hui-Hui Zhang,[a] Qu-Ran Wu,[a] Jun Gong,[a] Tong Liang,[a] Lu Gao,[b] Na-Na Xing,[a] Wen-Bin Liu,[c] Run-Lei Du,[a] Xiao-Dong Zhang[a]

College of Life Sciences, Wuhan University, Wuhan, China[a]; Department of Cardiology, Institute of Cardiovascular Disease, Union Hospital, Tongji Medical College, Hua Zhong University of Science and Technology, Wuhan, China[b]; College of Health Sciences and Nursing, Wuhan Polytechnic University, Wuhan, China[c]

Interleukin-1β (IL-1β) is a key proinflammatory cytokine that initiates several signaling cascades, including those involving CCAAT/enhancer binding proteins (C/EBPs). The mechanism by which IL-1β propagates a signal that activates C/EBP has remained elusive. Nemo-like kinase (NLK) is a mitogen-activated protein kinase (MAPK)-like kinase associated with many pathways and phenotypes that are not yet well understood. Using a luciferase reporter screen, we found that IL-1β-induced C/EBP activation was positively regulated by NLK. Overexpression of NLK activated C/EBP and potentiated IL-1β-triggered C/EBP activation, whereas knockdown or knockout of NLK had the opposite effect. NLK interacted with activating transcription factor 5 (ATF5) and inhibited the proteasome-dependent degradation of ATF5 in a kinase-independent manner. Consistently, NLK deficiency resulted in decreased levels of ATF5. NLK cooperated with ATF5 to activate C/EBP, whereas NLK could not activate C/EBP upon knockdown of ATF5. Moreover, TAK1, a downstream effector of IL-1β that acts upstream of NLK, mimicked the ability of NLK to stabilize ATF5 and activate C/EBP. Thus, our findings reveal the TAK1-NLK pathway as a novel regulator of basal or IL-1β-triggered C/EBP activation though stabilization of ATF5.

Nemo-like kinase (NLK), an evolutionarily conserved mitogen-activated protein kinase (MAPK)-related serine/threonine kinase, plays crucial roles in embryonic patterning, development, inflammation, and the DNA damage response (DDR) by modulating multiple signaling pathways (1–7). Several reports have suggested that NLK functions downstream of transforming growth factor β (TGF-β)-activated kinase 1 (TAK1), which is activated by TGF-β, Wnt, and interleukin-6 (IL-6) signaling (1–6). In response to these cascades, NLK phosphorylates several transcription factors, including STAT3, Lef-1, and c-Myb. Previously, we have shown that NLK plays a role in the DDR via p53 regulation (7). We also found that NLK negatively regulates nuclear factor kappa B (NF-κB) activity by disrupting the interaction between the TAK1 complex and IκB kinase β (IKK-β) (8). In invertebrates, NLK affects cell movement in *Drosophila* and cell fate determination in *Caenorhabditis elegans* (9, 10). In mice, NLK deficiency results in various abnormalities, such as neurological and morphological defects (11). Given the diverse pathways regulated by NLK and the complex and as yet poorly understood phenotypes in different models, the identification of additional pathways or mechanisms responsible for its functions is of great interest.

CCAAT/enhancer binding proteins (C/EBPs) are a family of transcription factors with structural and functional homology that have critical roles in numerous cellular responses, including cellular proliferation and differentiation, metabolism, immunity, and inflammatory processes (12–14). C/EBPs are involved in the interpretation of extracellular signals (15), including that initiated by the proinflammatory cytokine IL-1β (16–21), via a variety of mechanisms. IL-1β, the master cytokine in the IL-1 family, is associated with various cellular processes, including immunity, autophagy, and inflammation (22, 23). IL-1β exerts its effects mainly by activating NF-κB and MAPKs (22). Binding of IL-1β to its receptor, IL-1R, triggers a cascade that activates TAK1 to propagate downstream signaling (22, 24). However, the molecular mechanism by which the IL-1β cascade regulates C/EBP remains obscure (16–21).

Activating transcription factor 5 (ATF5), a member of the ATF/CREB protein family, contains a C-terminal bZIP domain and is involved in cellular proliferation, as well as differentiation, apoptosis, and the stress response (25). ATF5 was first identified as a partner of C/EBPγ (26), and a recent study demonstrated that ATF5 associates with C/EBPβ during 3T3-L1 differentiation (27). Several reports have suggested that ATF5 is inherently very unstable; however, it can be stabilized in response to a variety of stimuli, such as cisplatin (28), cadmium chloride ($CdCl_2$) (29), sodium arsenite ($NaAsO_2$) (30), and IL-1β (31).

To further understand the molecular function of NLK, we searched for new NLK-associated pathways via a luciferase reporter screen and identified C/EBP as a novel NLK-regulated pathway. Moreover, by developing a strategy called "knock-in affinity purification (AP)-mass spectrometry (MS)," we found that ATF5 is a novel NLK-interacting protein. We further revealed a signaling cascade in which TAK1-NLK potentiates IL-1β-triggered C/EBP activation. NLK decreases the proteasome-mediated degradation of ATF5 in a kinase-independent manner, which accounts for the potentiation of C/EBP activation by NLK. Further-

Received 4 December 2014 **Accepted** 10 December 2014

Accepted manuscript posted online 15 December 2014

Citation Zhang Z-Y, Li S-Z, Zhang H-H, Wu Q-R, Gong J, Liang T, Gao L, Xing N-N, Liu W-B, Du R-L, Zhang X-D. 2015. Stabilization of ATF5 by TAK1–Nemo-like kinase critically regulates the interleukin-1β-stimulated C/EBP signaling pathway. Mol Cell Biol 35:778–788. doi:10.1128/MCB.01228-14.

Address correspondence to Run-Lei Du, runleidu@whu.edu.cn, or Xiao-Dong Zhang, zhangxd@whu.edu.cn.

doi:10.1128/MCB.01228-14

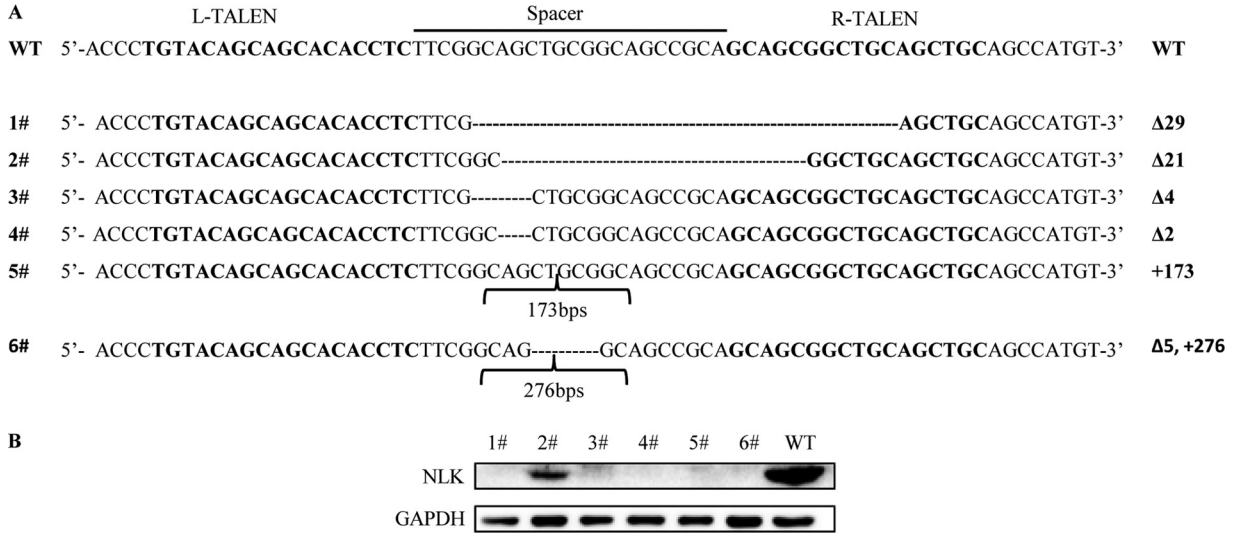

FIG 1 TALEN-induced gene knockout in *NLK*. (A) Sequencing results of the PCR fragments, revealing different mutations in the TALEN target site. Genomic DNA was isolated from cloned RKO cells to amplify the target site for sequencing. Sequences for WT and deletion mutants (1 to 6) are shown. (B) Western blot results for cells. Lysates were extracted from the indicated cells and examined by Western blot analysis with the indicated antibodies. GAPDH was the loading control.

more, both IL-1β and the subsequently activated TAK1 mimic the ability of NLK to stabilize ATF5 and activate C/EBP. Our findings uncover a new mechanism for the regulation of basal and IL-1β-induced ATF5 stabilization and C/EBP activation.

MATERIALS AND METHODS

Reagents and antibodies. Mouse monoclonal antibodies against Flag (Sigma), MYC (Roche), and GAPDH (glyceraldehyde-3-phosphate dehydrogenase) (CWBio), a rabbit monoclonal antibody against hemagglutinin (HA) (Cell Signaling Technology), a rabbit anti-NLK antibody (Bethyl), a rabbit anti-ATF5 antibody (Abcam), recombinant human IL-1β, (Biolegend), the protein translation inhibitor cycloheximide (Santa Cruz Biotechnology), the proteasome inhibitor MG132 (Selleckchem), the TAK1 inhibitor 5Z-7-oxozeaenol (TOCRIS), and luciferase reporters (Qiagen) were purchased from the indicated manufacturers. Mouse monoclonal anti-NLK was raised against human NLK expressed in bacteria.

Constructs. Plasmids expressing NLK and its mutants with the indicated tags were previously described (7). Mammalian expression plasmids containing Flag-ATF5 and its mutants were generated by cloning into pCDNA5/FRT/TO-Flag; HA-ATF5 and HA-luciferase (HA-Luc) were generated by cloning into pCDNA5/FRT/TO-HA. The vectors pEGF-C1 and pEGFP-N1 were used to generate enhanced green fluorescent protein (EGFP)-HA-ATF5 and ATF5-EGFP, respectively. All plasmids were constructed using standard molecular biology techniques. HA-tagged TAK1 and ubiquitin (Ub) were kindly provided by Hong-Bing Shu (Wuhan University).

Transfection and reporter assays. Cell transfection was performed using Turbofect (Thermo) according to the manufacturer's instructions. Where necessary, empty control vector was added to ensure that the total amounts of DNA transfected were equal across transfections. Luciferase assays were performed using a dual-luciferase assay kit (Promega). Firefly luciferase activities were normalized to *Renilla* luciferase (expressed via pRL-TK) activities.

Somatic-cell gene knock-in and knockout. HCT116 cells expressing 3× Flag-tagged endogenous NLK were established using recombinant adeno-associated virus (rAAV)-mediated homologous recombination (HR), and the CRISPR/Cas9 system was employed to enhance the HR rate. The details were as follows. The left and right homology arms contained in the pAAV-USER-Neo-LoxP-3×Flag vector were generated using the uracil-specific excision reagent (USER) system, and the resulting construct was used to produce rAAV virions in HEK293T cells as previously described (32). After transfection with CRISPR/Cas9 plasmids for 24 h, HCT116 cells were infected with rAAV for the next 48 h and then selected with 0.5 mg/ml Geneticin for approximately 2 weeks. Positive clones were identified from the Geneticin-resistant clones by genomic PCR using primers derived from the neomycin resistance gene and the upstream region of the left homology arm. The desired clones were also confirmed by Western blot analysis. Finally, correct knock-in clones were infected with Cre recombinase-transducing adenovirus to delete the neomycin selection marker. The HCT116 $NLK^{-/-}$ cells were generated using AAV-mediated HR, the details of which were described in our previous report (8). The NLK-deficient RKO cells were generated using TALEN-mediated knockout.

Flag affinity purification and mass spectrometry. The NLK-3× Flag knock-in HCT116 cells and control cells (2×10^8 each) were lysed with radioimmunoprecipitation assay (RIPA) lysis buffer (50 mM Tris [pH 7.4], 1 mM EDTA [pH 8.0], 150 mM NaCl, 10% glycerol, 1% NP-40, 5 mM NaF, and protease inhibitor cocktail [Roche]). Anti-Flag beads (Sigma; 150 μl) were prepared by washing them twice with Flag lysis buffer and then adding them to the cell supernatants, which were rocked for 5 h at 4°C. Next, the beads were spun down and washed five times with Flag lysis buffer. Flag peptide (500 μg/ml; 100 μl each) was used to elute the protein complex. Finally, 15 μl of 4× SDS loading buffer was added to the final elution, which was boiled down to 60 μl. Silver staining was performed according to the manufacturer's instructions (Sigma).

Coimmunoprecipitation and Western blotting. For exogenous coimmunoprecipitation experiments, transfected 293 cells (1×10^6) were lysed in 400 μl of NP-40 lysis buffer (30 mM Tris [pH 7.4], 150 mM NaCl, 1% NP-40) with proteinase inhibitor cocktail (Roche). For endogenous coimmunoprecipitation experiments, 293T cells (1×10^8) were lysed. The supernatants were incubated with the indicated antibodies and protein G beads (Roche) at 4°C for 3 h and then washed three times with buffer containing 0.3 M NaCl. The precipitates were analyzed using standard Western blotting procedures. The bands were quantified using Image Lab 3.0 (Bio-Rad).

Fluorescent confocal microscopy. 3× Flag knock-in HCT116 cells were cultured on coverslips and transfected with the HA-ATF5 expression

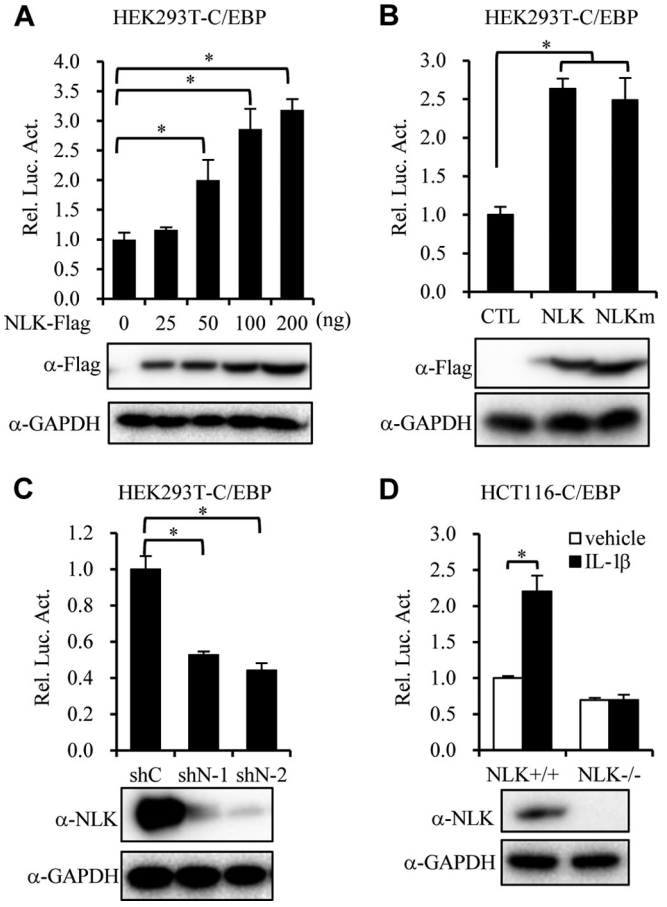

FIG 2 NLK activates basal and IL-1β-induced C/EBP activation. (A) Effects of NLK on C/EBP activation in HEK293T cells. HEK293T cells (approximately 1×10^5) were transfected with a C/EBP luciferase reporter (100 ng) and the indicated amounts of NLK-Flag plasmids, and reporter assays were performed 24 h after transfection. The expression of the transfected plasmids was examined by Western blotting. GAPDH was used as a loading control. (B) Effects of NLK and NLKm on C/EBP activation in HEK293T cells. The experiments were performed as described for panel A. (C) Effects of NLK knockdown on C/EBP activation. NLK expression was silenced using shRNAs (shN-1 and shN-2). The experiments were performed as for panel A. (D) Effects of NLK knockout on IL-1β-induced C/EBP activation. HCT116 $NLK^{+/+}$ cells and HCT116 $NLK^{-/-}$ cells (approximately 1×10^5) were transfected with a C/EBP reporter. Twenty-four hours after transfection, the cells were treated with IL-1β (1 ng/ml) or vehicle control for the next 12 h, after which the reporter assays were conducted. The graphs show means and SD; $n = 3$. The asterisks indicate a significant difference ($P < 0.05$) calculated by one-way analysis of variance followed by Tukey's multiple-comparison test.

plasmid. After 36 h, the cells were fixed with 4% paraformaldehyde and permeabilized with 0.1% Triton X-100 in phosphate-buffered saline (PBS). Then, the cells were washed with PBS and blocked with 5% bovine serum albumin (BSA) in PBS for 30 min. To visualize the expression of NLK-3× Flag and HA-ATF5, mouse anti-Flag antibody and rabbit anti-HA antibody were used as primary antibodies, and mouse Alexa Fluor 594-conjugated and rabbit Alexa Fluor 488-conjugated antibodies (Invitrogen) were used as secondary antibodies. DAPI (4′,6-diamidino-2-phenylindole) was used to stain the nucleus. Finally, the slips were observed and digitally photographed using a confocal microscope under a 60× oil objective.

RNA isolation and quantitative real-time PCR (qPCR). RNA isolation and first-strand cDNA synthesis were performed as previously described (8). The mRNA level of *ATF5* was normalized to *GAPDH* mRNA. The sequences of the primers were as follows: *ATF5*, 5′-GCCATGGAGTCTTCCACTTT-3′ (forward) and 5′-CACTGATGGCAACAGGAGAG-3′ (reverse); *GAPDH*, 5′-GAGTCAACGGATTTGGTCGT-3′ (forward) and 5′-GACAAGCTTCCCGTTCTCAG-3′ (reverse).

Generation of NLK or NLKm reexpression stable cell lines. To perform rescue experiments, NLK and the kinase-dead mutant NLK (lysine [K] 155 methionine [M], referred to here as NLKm) were reexpressed in the cells by lentiviral infection. MYC-NLK and MYC-NLKm expression plasmids were produced using the pHAGE-CMV-MCS-PGK-puro backbone. HEK293T cells were transfected with these plasmids and lentiviral packaging vectors. At 48 h posttransfection, the viral supernatants were filtered and added to HCT116 wild-type (WT) or HCT116 $NLK^{-/-}$ cells in the presence of Polybrene (6 μg/ml). The transduced cells were selected by puromycin treatment for 2 weeks before additional experiments were performed.

Phos-tag assay. SDS-PAGE gels (10% polyacrylamide) containing 25 mM Phos-tag acrylamide (Wako Chemicals), and 100 mM $MnCl_2$ were used to detect phosphorylated proteins. After electrophoresis, the Phos-tag acrylamide gels were washed according to the manufacturer's protocol to eliminate Mn^{2+}. The remainder of the protocol was carried out following standard Western blotting procedures.

RNA interference (RNAi), TALEN, and CRISPR/Cas9 experiments. Double-stranded oligonucleotides corresponding to the target sequences were cloned into the pLKO.1 vector (Addgene). The sequences were as follows: human NLK 1 (shNLK-1 or shN-1), 5′-ACCTCCACACATTGACTATTT-3′; human NLK 2 (shNLK-2 or shN-2), 5′-CGGATAGACCTATTGGATATG-3′; human ATF5 1 (shATF5-1 or shA-1), 5′-TGGATGACTGAGCGAGTTGAT-3′; and human ATF5 2 (shATF5-2 or shA-2), 5′-GCTGGAACAGATGGAAGACTT-3′. The TALENs for NLK knockout in RKO cells were assembled using our in-house-developed USER method. The backbones were modified from pCS2-PEAS and pCS2-PERR (33). The target sites and the spacer were as indicated (Fig. 1). The guide RNA (gRNA) targeting the stop codon (in boldface) region of NLK had the following sequence: 5′-CTCCTCTGGTGTGGGAG**TGA**-3′. The backbone for gRNA cloning was PX459 (34).

Denaturing immunoprecipitation and ubiquitination analysis. To detect the effect of NLK on ATF5 ubiquitination, denaturing immunoprecipitation and ubiquitination analysis were performed as previously described (35). HEK293T cells were transfected with the indicated plasmids, and at 36 h posttransfection, the cells were washed with PBS and lysed with 1 volume of SDS lysis buffer (10% SDS in PBS). The lysates were heated at 95°C, and then, 2 volumes of modified RIPA buffer (50 mM Tris-HCl [pH 7.4], 150 mM NaCl, 1 mM EDTA, and protease inhibitor) was added to the lysates. Then, the lysates were cooled on ice for 1 h and centrifuged at 18,000 × *g* for 30 min at 4°C. Finally, the supernatant was subjected to anti-Flag immunoprecipitation and Western blot analysis.

Statistical analyses. The data are expressed as means and standard deviations (SD). Statistical analyses were performed using Prism 5.0 (GraphPad Software, San Diego, CA). Significant differences ($P < 0.05$) were calculated by one-way analysis of variance followed by Tukey's multiple-comparison test.

RESULTS

NLK activates the C/EBP pathway. In an attempt to identify novel NLK-associated signaling pathways, we screened the Cignal 45-pathway reporter from Qiagen using luciferase assays. We found that NLK activated the C/EBP pathway. As shown in (Fig. 2A), overexpression of NLK promoted C/EBP activation in HEK293T cells in a dose-dependent manner. Furthermore, NLK also activated C/EBP in HCT116 cells in a manner that was only partially dependent on its kinase activity (Fig. 2B). To examine the regulation of C/EBP in a more physiological context, we knocked down NLK in HEK293T cells and found that C/EBP activation was inhibited (Fig. 2C). As reported previously (16), IL-1β caused an

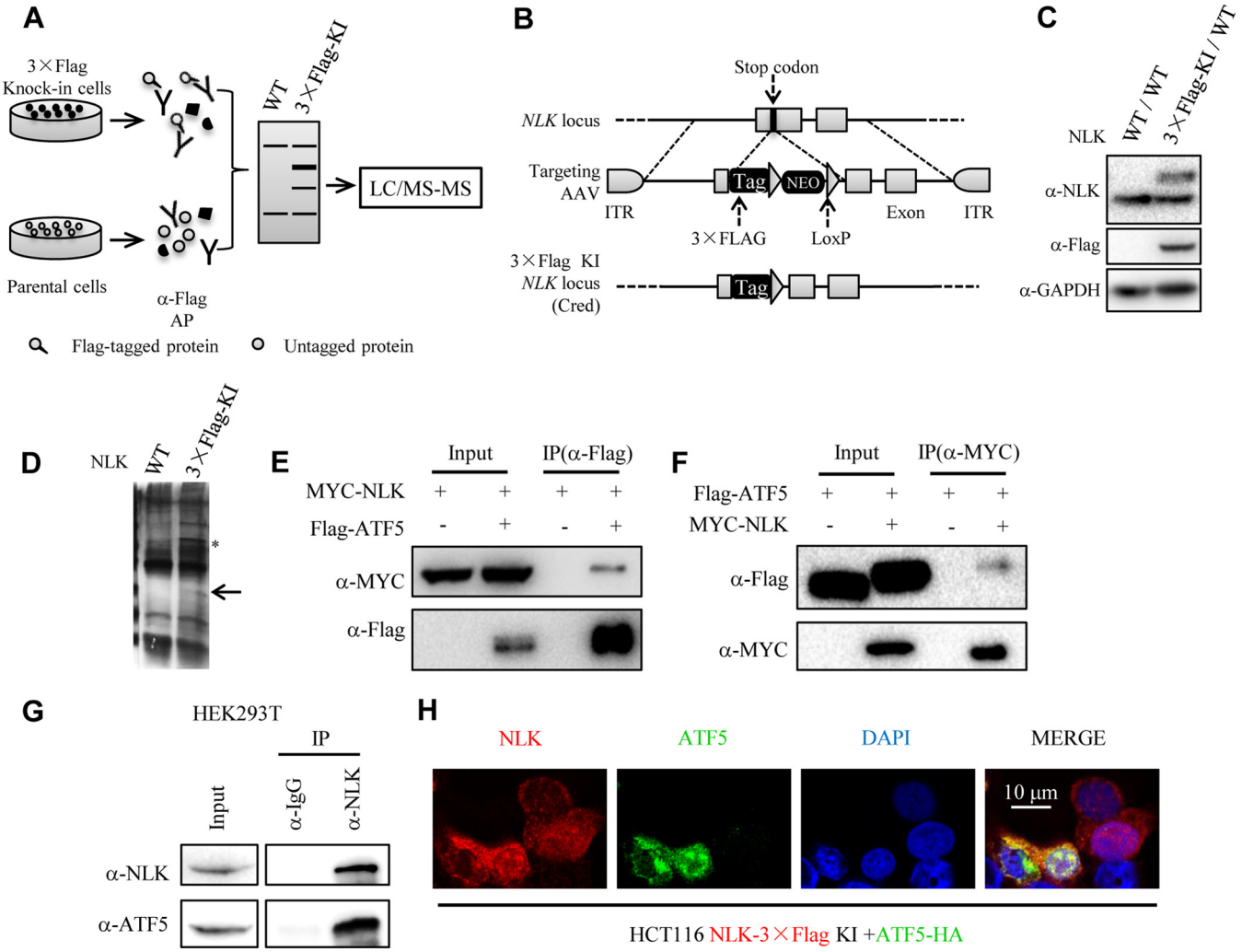

FIG 3 Identification of ATF5 as a novel NLK-interacting protein by knock-in AP-MS. (A) Workflow of the knock-in AP-MS strategy. LC/MS-MS, liquid chromatography-tandem MS. α, anti. (B) Schematic diagram of the NLK-3× Flag knock-in. ITR, inverted terminal repeat; NEO, neomycin. (C) Confirmation that 3× Flag was knocked-in to the C terminus of the endogenous NLK locus. Cell lysates from WT HCT116 and HCT116 $NLK^{WT/3\times Flag}$ cells were extracted and examined by Western blotting with the indicated antibodies. (D) Silver staining of the NLK-3× Flag-containing protein complexes and untagged controls. HCT116 $NLK^{WT/3\times Flag}$ and HCT116 $NLK^{WT/WT}$ cells (2×10^8 each) were lysed and subsequently examined by AP and silver staining. (E and F) Interaction between exogenous NLK and ATF5. HEK293T cells were transiently transfected with the indicated constructs. Anti-FLAG (E) or anti-MYC (F) immunoprecipitates (IP) were immunoblotted with anti-Flag (ATF5) or anti-MYC (NLK) antibodies, respectively. (G) Interaction between endogenous NLK and ATF5. HEK293T cell lysates were immunoprecipitated using anti-NLK or IgG antibodies, followed by Western blotting with anti-NLK and anti-ATF5 antibodies. Cell lysates (5% input) were used for Western blotting. (H) Colocalization of endogenous NLK and HA-ATF5. HCT116 NLK-3× Flag knock-in cells (5×10^4) were transiently transfected with 500 ng of HA-ATF5 plasmid. Thirty-six hours after transfection, fluorescence confocal microscopy analysis was performed.

approximately 3-fold increase in the activation of C/EBP, and this effect was almost completely abolished when NLK was knocked out (Fig. 2D). Taken together, these data suggest that NLK positively regulates C/EBP signaling.

Identification of ATF5 as a novel NLK-interacting protein by knock-in AP-MS. In another effort to identify novel NLK-interacting proteins in a physiological context, we developed a strategy referred to as knock-in AP-MS (Fig. 3A). To avoid the nonphysiological overexpression of the epitope-tagged bait protein, we expressed a triple-Flag-tagged NLK from the endogenous locus by AAV-mediated somatic-cell gene knock-in in the human colon cancer cell line HCT116 (Fig. 3B). As shown in Fig. 3C, endogenous NLK was successfully tagged with 3× Flag, which was determined by Western blot analysis of cell extracts from the knock-in and control cells (the untagged parental cells) with both anti-Flag and anti-NLK antibodies. Then, an AP-MS experiment was performed with anti-Flag beads using the knock-in cells in parallel with parental control cells (Fig. 3D). The NLK-Flag-containing protein complexes and untagged control were purified and separated on SDS-PAGE. The resulting bands were visualized using silver staining and excised from the gel for MS analysis. The MS result showed that the protein band with an apparent molecular mass of 35 kDa contained several proteins (Table 1).

Among the possible NLK-interacting proteins, cyclic-AMP-dependent ATF5 (Table 1, boldface) was notable because it has been reported to interact with C/EBP family proteins, such as C/EBPγ and C/EBPβ (27, 36), and NLK has been reported to interact with and regulate several transcription factors (37). To

TABLE 1 Proteins involved in the affinity-purified band[a]

Accession no.	Description	Score
P05141	ADP/ATP translocase 2	834.16
P12236	ADP/ATP translocase 3	727.82
P12235	ADP/ATP translocase 1	656.03
Q6NUK1	Isoform B of phosphate carrier protein, mitochondrial	223.55
Q9Y2D1	**Cyclic-AMP-dependent transcription factor ATF5**	**190.40**
P83010	13-kDa protein	180.02
P06309	Similar to Ig kappa chain V-II region GM607 precursor	162.11
B4DDU2	cDNA FLJ60097; highly similar to tubulin alpha-ubiquitous chain	110.84
Q9BQE3	Tubulin alpha-1C chain	104.54
T0MHB5	Mitochondrial 2-oxoglutarate/malate carrier protein isoform 2	90.31
Q9BQA1	Methylosome protein 50	71.78
P04264	Keratin, type II cytoskeletal 1	57.47

[a] Affinity-purified proteins were identified by MS analysis, and the detailed information is summarized in the table. Accession numbers are those from the UniprotKB database (http://www.uniprot.org/mapping/); the score is Mascot score.

verify the interaction between NLK and ATF5, we transfected HEK293T cells with Flag-ATF5 and MYC-NLK and performed coimmunoprecipitation analysis. Immunoblotting of the Flag immunoprecipitate from the cotransfected cells using an anti-MYC antibody showed that Flag-ATF5 associated with MYC-NLK (Fig. 3E). A similar result was obtained using MYC immunoprecipitate and anti-Flag probing (Fig. 3F). To further confirm the physiological interaction, endogenous coimmunoprecipitation was performed and showed that endogenous NLK interacted with ATF5 (Fig. 3G). Additionally, endogenous 3× Flag-tagged NLK colocalized with transfected HA-ATF5 (Fig. 3H). These results demonstrate that NLK interacts with ATF5.

ATF5 is necessary for NLK-mediated activation of C/EBP. Given that ATF5 enhances C/EBPβ activation and interacts with C/EBPγ (27, 36), we reasoned that NLK might positively regulate C/EBP via ATF5. As expected, forced expression of ATF5 activated C/EBP in a dose-dependent fashion (Fig. 4A), and silencing of ATF5 using RNAi inhibited C/EBP activation (Fig. 4B). To determine the relationship between NLK and ATF5 in the regulation of the C/EBP signaling pathway, we cotransfected NLK and ATF5 or vector control and performed a C/EBP-luciferase reporter assay. As shown in Fig. 4C, the expression of NLK and ATF5 synergistically stimulated the C/EBP reporter. Furthermore, NLK did not activate C/EBP when ATF5 was knocked down (Fig. 4D). Taken together, these data suggest that ATF5 is necessary for NLK-mediated potentiation of C/EBP activation.

Phosphorylation of ATF5 by NLK cannot account for C/EBP activation. To elucidate the mechanism by which NLK cooperates with ATF5 to regulate C/EBP signaling, we coexpressed ATF5 with NLK in cells. Notably, when ATF5 was coexpressed with NLK, two events were observed: the ATF5 bands appeared at a higher molecular weight in Western blot analyses, and the ATF5 protein level increased (Fig. 5A). Considering that NLK is known to be a kinase and to interact with ATF5, we speculated that the observed migration shift of ATF5 may be due to phosphorylation of the protein, and we tested this hypothesis first. As expected, only wild-type NLK, but not NLKm, altered the migration of ATF5 (Fig. 5A). Furthermore, the upward shift in ATF5 migration induced by NLK was lowered by λ protein phosphatase (λ-PPase) treatment (Fig. 5A, lane 4). To further confirm that NLK can phosphorylate ATF5, Phos-tag SDS-PAGE, which significantly retards the migration of phosphorylated proteins, was employed (38). Both human and mouse ATF5 exhibited significant migration retardation in Phos-tag gels when coexpressed with NLK (Fig. 5B). To elucidate the sites on ATF5 that were phosphorylated by NLK, we employed the kinase prediction algorithms GPS 2.1 (39) and Scansites 2.0 (40). ATF5 contained several sites, including four proline (P)-directed serine/threonine (S/T) residues (92, 94, 126, and 190) and two non-P-directed S/T residues (144 and 147), that were predicted MAPK substrates (Fig. 5C). With this information, we mutated one or more potential sites from S/T to alanine (A), which cannot be phosphorylated. The transient-transfection and immunoblotting results showed that ATF5-4A and ATF5-6A no longer exhibited migration retardation when coexpressed with

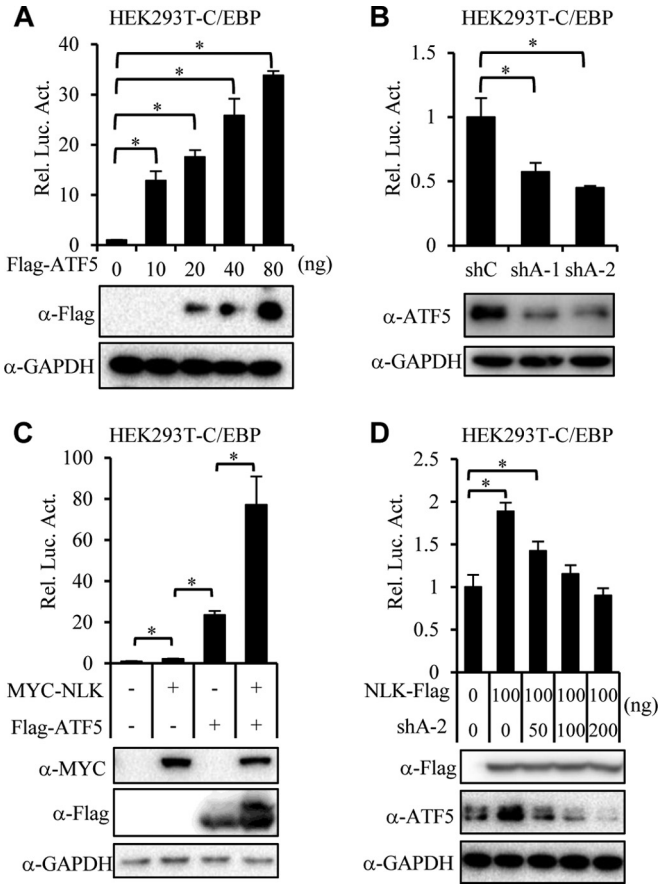

FIG 4 ATF5 is necessary for NLK-mediated activation of C/EBP. (A) Effects of ATF5 on C/EBP activation. HEK293T cells (1×10^5) were cotransfected with C/EBP reporter (100 ng) and the indicated amounts of plasmids. Twenty-four hours posttransfection, reporter assays were performed. The expression of the transfected plasmids was detected by Western blotting. (B) Effects of ATF5 knockdown on C/EBP activation. The experiments were performed as for panel A. (C) Synergistic effects of NLK and ATF5 on C/EBP activation. The experiments were performed as for panel A. (D) Effects of ATF5 deficiency on NLK induction of C/EBP. The experiments were performed as for panel A. The graphs present means and SD; $n = 3$. The asterisks indicate a significant difference ($P < 0.05$) calculated by one-way analysis of variance followed by Tukey's multiple-comparison test. α, anti.

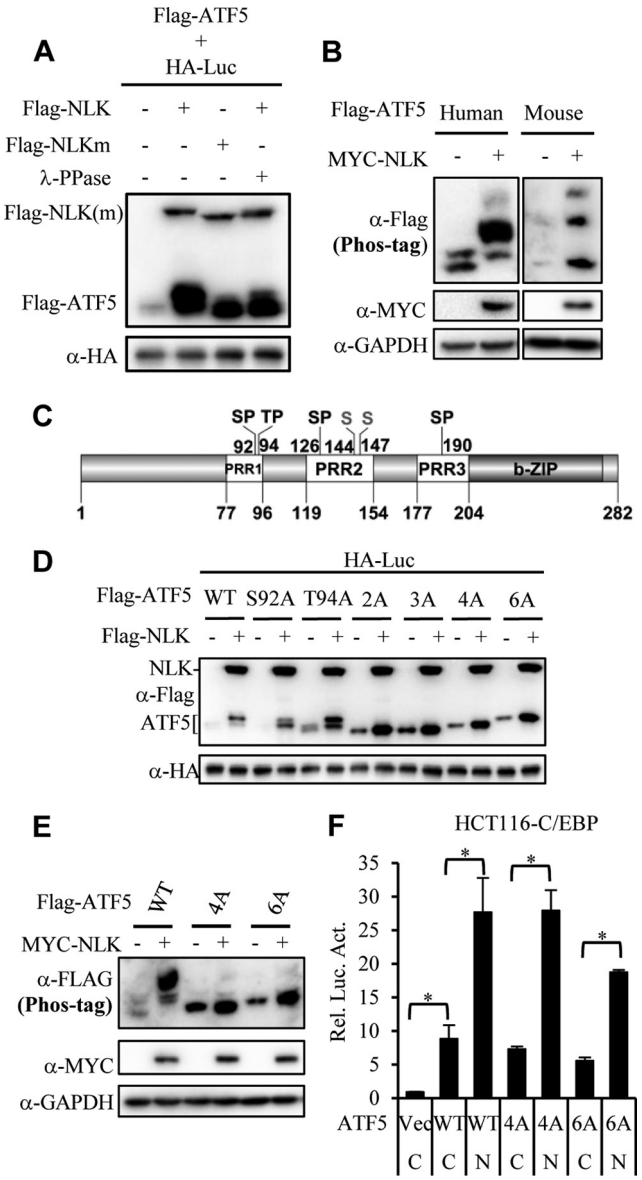

FIG 5 Phosphorylation of ATF5 by NLK cannot account for C/EBP activation. (A and B) NLK phosphorylates ATF5 and increases its protein expression. HEK293T cells (4×10^5) were transfected with the indicated plasmids. (A) Thirty-six hours after transfection, the cells were lysed and treated with λ-PPase or control, and Western blot analysis was performed using the indicated antibodies and HA-Luc for normalization. α, anti. (B) HEK293T cells (4×10^5) were transfected with the indicated plasmids. Thirty-six hours after transfection, the cells were lysed, and the lysates were analyzed using the Phos-tag assay. (C) Diagram of the potential MAPK phosphorylation sites within ATF5. There are four P-directed S/T residues (92, 94, 126, and 190) and two non-P-directed S/T residues (144 and 147). ATF5-3A is an ATF5 mutant with residues 92, 94, and 126 altered to A. In ATF5-4A, all four P-directed S/T residues were mutated to A, and in ATF5-6A, all predicted S/T residues were mutated to A. (D and E) Several sites within ATF5 that are predicted to be phosphorylated by NLK. HEK293T cells (4×10^5) were transfected with the indicated plasmids. At 36 h posttransfection, the cells were lysed, and then, the lysates were analyzed by Western blotting (D) and the Phos-tag assay (E). (F) ATF5 activates C/EBP and cooperates with NLK to induce C/EBP activation. HEK293T cells (1×10^5) were cotransfected with the C/EBP reporter plasmid (100 ng) and other indicated plasmids (Vec, vector of ATF5; C, vector of NLK; N, NLK-expressing plasmid). Twenty-four hours after transfection, reporter assays were performed. The graphs present means and SD; $n = 3$. The asterisks indicate a significant difference ($P < 0.05$) calculated by one-way analysis of variance followed by Tukey's multiple-comparison test.

NLK (Fig. 5D). To further confirm these results, Phos-tag SDS-PAGE was employed again. The Phos-tag Western blotting results further indicated that the ATF5-4A and ATF5-6A mutants were no longer phosphorylated by NLK (Fig. 5E). Nevertheless, luciferase reporter assays showed that the ATF5-6A mutant, which was not phosphorylated by NLK, significantly activated C/EBP (Fig. 5F). Together, these results suggest that NLK can promote ATF5 phosphorylation at several residues; however, this phosphorylation is not required for NLK to positively regulate C/EBP.

NLK stabilizes ATF5 at the protein level in a kinase-independent manner. The above-mentioned results indicate that, along with phosphorylation by NLK, ATF5 protein expression was higher when it was coexpressed with NLK (Fig. 5A and D). However, the latter event does not appear to rely on the former, as the kinase-dead mutant NLKm also increased ATF5 protein levels (Fig. 5A), which is consistent with the observation that NLK markedly potentiated the expression of the ATF5-4A and ATF5-6A mutants (Fig. 5D and E). To verify that NLK enhanced ATF5 expression posttranslationally, cycloheximide (CHX), an inhibitor of protein translation, was employed to measure the half-life of ATF5 decay. The results showed that exogenous expression of NLK prolonged the half-life of transfected ATF5 (Fig. 6A). To examine whether endogenous NLK was involved in regulating ATF5, we generated NLK-deficient HCT116 and RKO cells using AAV-mediated homologous recombination and TALEN technology (Fig. 1), respectively. Western blot analysis showed that endogenous ATF5 protein levels were reduced in both HCT116 $NLK^{-/-}$ and RKO $NLK^{-/-}$ cells compared with the corresponding wild-type parental cells (Fig. 6B) without the occurrence of similar changes in mRNA levels (Fig. 6C). Furthermore, reexpression of NLK or NLKm rescued the downregulated ATF5 protein level (Fig. 6D), which further confirmed that NLK stabilized ATF5 in a kinase-independent manner. Consistently, the half-life of endogenous ATF5 was prolonged in NLK-overexpressing HEK293T cells compared with the empty-vector-expressing cells and shortened in NLK-deficient HCT116 cells compared with the wild-type cells (Fig. 6E and F). These results demonstrate that NLK stabilizes ATF5 at the protein level in a kinase-independent manner.

Inhibition of proteasome-mediated degradation of ATF5 by NLK is involved in C/EBP regulation. Posttranslational intracellular degradation of proteins occurs mainly through lysosome- and/or Ub-proteasome-mediated proteolysis (41). To determine how NLK affected the proteolysis of ATF5, MG132 and NH_4Cl were used to block proteasomes and lysosomes, respectively. The NLK-mediated stabilization of ATF5 was inhibited by MG132 but not NH_4Cl (Fig. 6G). Thus, these results indicate that NLK mediated ATF5 stabilization through inhibition of the proteasome pathway. In addition, the ubiquitination analysis was extended by first immunoprecipitating ATF5 under denaturing conditions and immunoblotting the detected HA-Ub. These analyses showed that both NLK and NLKm were able to inhibit the ubiquitination of ATF5 (Fig. 6H). Furthermore, the downregulation of C/EBP activity in HCT116 $NLK^{-/-}$ cells was rescued by the reexpression of NLK and NLKm (Fig. 7E). Collectively, these data suggest that inhibition of the proteasome-mediated degradation of ATF5 by NLK is involved in the regulation of C/EBP.

The N-terminal residues of ATF5 are required for NLK-mediated phosphorylation and stabilization. It has been reported that N-terminal residues play an important role in ATF5 stability

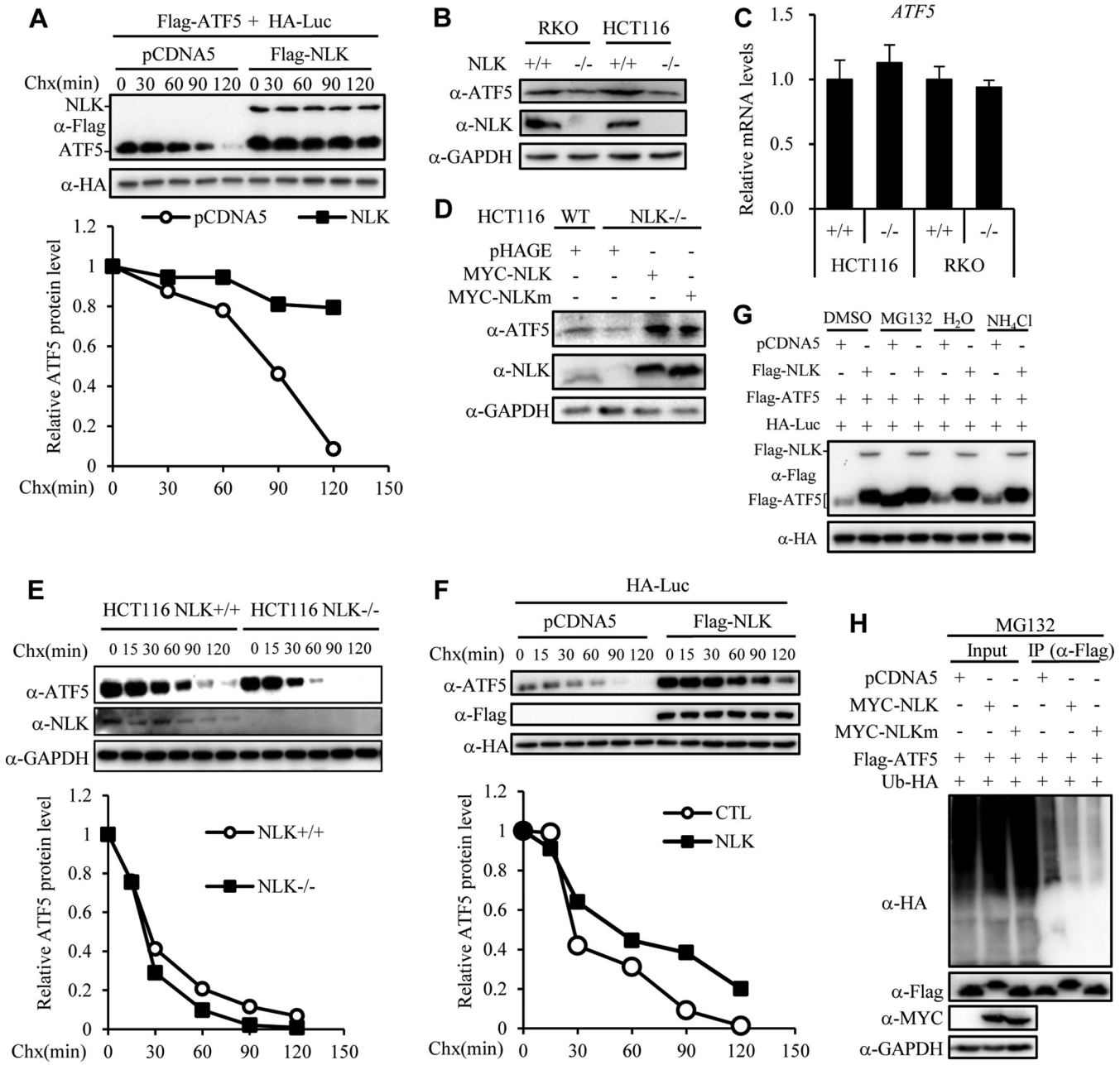

FIG 6 Inhibition of proteasome-mediated degradation of ATF5 by NLK is involved in C/EBP regulation. (A) Exogenous expression of NLK prolongs the half-life of exogenous ATF5. HEK293T cells (4×10^5) were transfected with the indicated plasmids. Thirty hours after transfection, the cells were treated with 50 μg/ml cycloheximide (Chx) for the indicated times, and the cell lysates were analyzed by Western blotting with the indicated antibodies. Protein expression was normalized to HA-Luc expression. The quantified data are relative to the corresponding time zero. α, anti. (B) Knockout of NLK decreases endogenous ATF5 protein levels in HCT116 and RKO cells. The indicated cell lysates were extracted and examined by Western blotting with the indicated antibodies. (C) NLK knockout does not affect the mRNA levels of ATF5 in HCT116 or RKO cells. The expression levels were normalized to those of the GAPDH housekeeping gene and compared with those of the wild-type controls. (D) Effects of NLK or NLKm reexpression on ATF5 stability in HCT116 $NLK^{-/-}$ cells. The indicated cell lysates were extracted and examined by Western blot analysis with the indicated antibodies. (E and F) Effects of NLK overexpression (E) or NLK deficiency (F) on the half-life of endogenous ATF5. The experiments were performed as for panel A. (G) Effects of MG132 and NH_4Cl on NLK-mediated ATF5 stabilization. HEK293T cells (4×10^5) were transfected with the indicated plasmids. Thirty hours after transfection, the cells were treated with 10 μM MG132 or 50 mM NH_4Cl for 8 h, and then the cell lysates were analyzed by Western blotting with the indicated antibodies. (H) Effects of NLK on ATF5 ubiquitination. HEK293T cells (2×10^6) were cotransfected with the indicated plasmids. Thirty-six hours posttransfection, the cells were subjected to denaturing immunoprecipitation using anti-Flag antibody, followed by Western blot analysis with the indicated antibodies.

(31). Accordingly, truncated ATF5 was overexpressed with NLK to determine whether the N-terminal residues were required for the NLK-mediated stabilization of ATF5. The result showed that ATF5 lacking the first 130 N-terminal amino acids, which could not be stabilized by NLK, was more stable than wild-type ATF5 (Fig. 8A). Because the N terminus was important for NLK-mediated stabilization of ATF5, we found that NLK did not stabilize the full-length ATF5 when a large tag (EGFP) was appended to its N

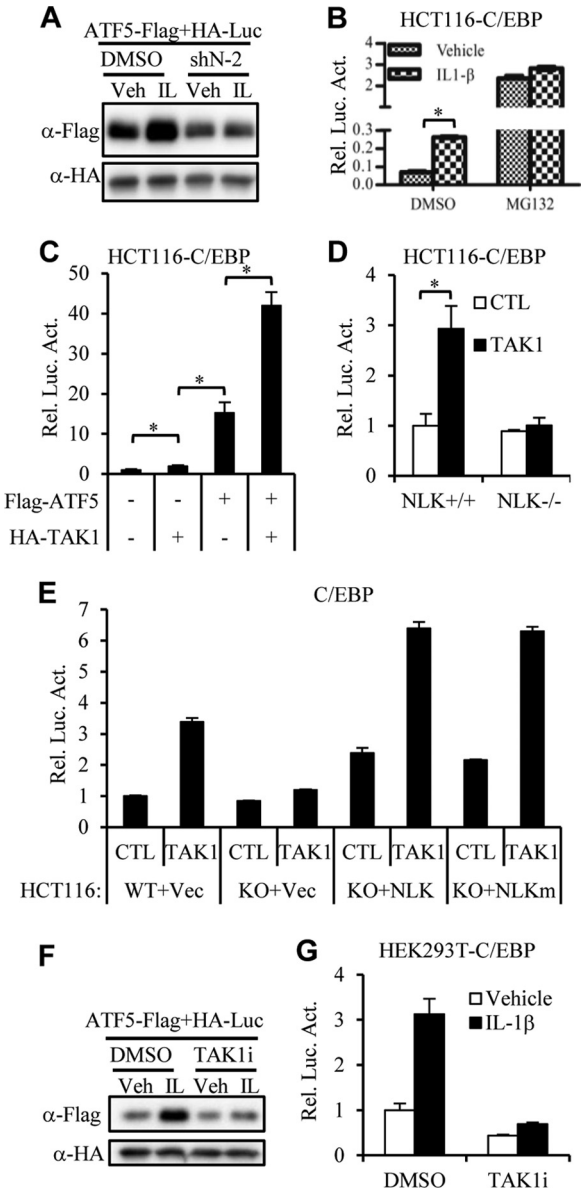

FIG 7 IL-1β stabilizes ATF5 and activates C/EBP through TAK1-NLK. (A) Effects of NLK silencing on IL-1β-induced ATF5 stabilization. HEK293T cells (4×10^5) were transfected with the indicated plasmids. Twenty-four hours after transfection, the cells were treated with vehicle (Veh) or 2 ng/ml IL-1β (IL) for 12 h, followed by Western blot analysis of cell lysates with the indicated antibodies. DMSO, dimethyl sulfoxide. α, anti. (B) Effects of MG132 on IL-1β-triggered C/EBP activation. HCT116 cells (1×10^5) were transfected with C/EBP reporter plasmid (200 ng). Twenty-four hours after transfection, the cells were treated with 2 ng/ml IL-1β or vehicle, together with 5 μM MG132 or DMSO for 12 h. (C) TAK1 mimics the ability of NLK to cooperate with ATF5 to elicit C/EBP activation. HCT116 cells (1×10^5) were cotransfected with C/EBP reporter (100 ng) and the indicated amounts of plasmids. Twenty-four hours after transfection, reporter assays were performed. (D) Effects of NLK knockout on TAK1-induced C/EBP activation. HCT116 $NLK^{+/+}$ and HCT116 $NLK^{-/-}$ cells (approximately 1×10^5) were cotransfected with C/EBP reporter (200 ng) and TAK1 (100 ng) or empty vector. Twenty-four hours after transfection, reporter assays were performed. (E) Effects of NLK or NLKm reexpression on TAK1-mediated C/EBP activation. The indicated cells were transfected with the reporter. Twenty-four hours posttransfection, a luciferase assay was performed. (F and G) Effects of TAK1i (5Z-7-oxozeaenol) treatment on ATF5 stabilization and C/EBP activation. HEK293T cells were transfected with the indicated plasmids. Twelve hours posttransfection, the cells were treated with IL (2 ng/ml) or vehicle, together with TAK1i (100 nM) or DMSO for 12 h. Finally, the cells were subjected to Western blotting with the indicated antibodies (F) or to luciferase assay (G). The graphs present means and SD. The asterisks indicate a significant difference ($P < 0.05$) calculated by one-way analysis of variance followed by Tukey's multiple-comparison test.

terminus (Fig. 8B). However, appending EGFP to the C terminus did not affect NLK-mediated stabilization of ATF5 (Fig. 8C). Moreover, ATF5 lacking the N terminus did not activate C/EBP or cooperate with NLK to potentiate C/EBP activation (Fig. 8D). Consistently, ATF5-EGFP, which was stabilized by NLK, but not EGFP-HA-ATF5, which was not stabilized by NLK, exhibited synergistic effects on C/EBP activation when coexpressed with NLK (Fig. 8E). These observations indicate that N-terminal residues within ATF5 confer the NLK-mediated ATF5 stabilization and C/EBP activation.

IL-1β and TAK1 function upstream of NLK and ATF5 to activate C/EBP. It has been reported that IL-1β also regulates the stability of ATF5 via the N-terminal domain of the latter (31), and IL-1β also activates C/EBP signaling (including C/EBPβ and C/EBPδ signaling) (16–21). Hence, we speculated that IL-1β might act upstream of NLK to stabilize ATF5 and to activate C/EBP signaling. ATF5 protein levels were increased when we treated 293T cells with IL-1β compared with vehicle (control); however, IL-1β did not further stabilize ATF5 when NLK was knocked down (Fig. 7A). Similarly, the C/EBP reporter assay showed that IL-1β activated C/EBP approximately 2.2-fold in HCT116 $NLK^{+/+}$ cells, and this effect was almost completely abolished in HCT116 $NLK^{-/-}$ cells (Fig. 2D). Furthermore, the induction of C/EBP by IL-1β in HCT116 cells was weakened when proteasomes were blocked by MG132 treatment (Fig. 7B), suggesting that ATF5 stabilization is critical for C/EBP activation. In summary, these results indicate that IL-1β functions upstream of NLK to stabilize ATF5 and activate C/EBP.

Because several studies showed that TAK1 is an upstream regulator of NLK (2, 3, 5, 37, 42, 43) and a downstream effector of IL-1β-triggered signaling (22, 23, 44–46), we examined the roles of TAK1 in ATF5 stabilization and C/EBP activation. In accordance with the results of the NLK experiments, overexpression of TAK1 activated C/EBP in cooperation with ATF5 in HEK293T cells (Fig. 7C). Consistently, TAK1 activated C/EBP in HCT116 $NLK^{+/+}$ cells by approximately 3-fold, and this effect was almost completely abolished in HCT116 $NLK^{-/-}$ cells (Fig. 7D) and was rescued by the reexpression of NLK or NLKm (Fig. 7E). Furthermore, the IL-1β-induced ATF5 stabilization and C/EBP activation were blocked by TAK1 inhibitor (TAK1i) treatment (Fig. 7F and G). In summary, these observations suggest that IL-1β stabilizes ATF5 and activates C/EBP through TAK1-NLK.

DISCUSSION

It has been well documented that the propagation of IL-1β signaling mainly depends on MAPKs and their downstream effectors, which activate multiple transcription factors (22, 23). Several reports have suggested that C/EBP is activated by IL-1β stimulation (16–21); however, the underlying mechanism has not been fully described. In this study, we identified NLK, a MAPK-related kinase, as a positive regulator of basal and IL-1β-triggered C/EBP activation. Overexpression of NLK activated C/EBP and potentiated IL-1β-induced activation of C/EBP, whereas knockout or knockdown of NLK had the opposite effect. Consistent with the

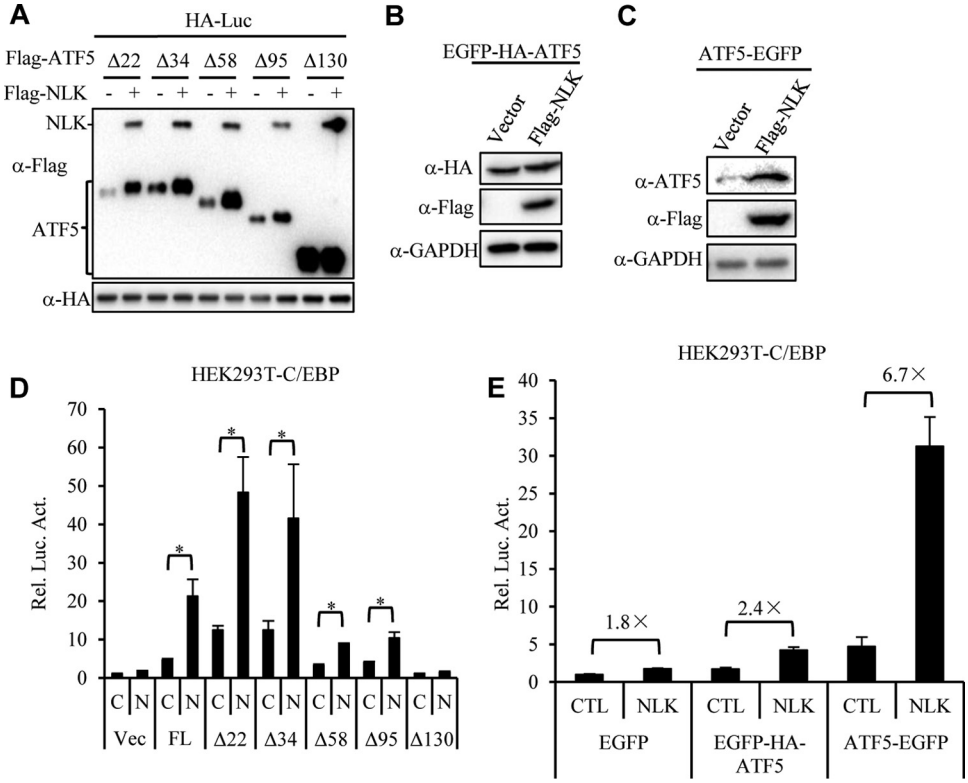

FIG 8 The N terminus of ATF5 is important for NLK-mediated ATF5 functions. (A) The N terminus of ATF5 confers NLK-mediated stabilization of ATF5. HEK293T cells (4×10^5) were transfected with the indicated plasmids (Δ22 and Δ34 etc., represent ATF5 lacking the last 22 and 34 amino acids, etc., at the C terminus). Thirty-six hours after transfection, the cells were lysed, and the lysates were analyzed by Western blotting with the indicated antibodies. α, anti. (B and C) A large N- or C-terminal tag (EGFP) on ATF5 affects its ability to be stabilized by NLK. The experiments were performed as for panel A. (D) Effects of N-terminal deletion of ATF5 on C/EBP activation. HEK293T cells (1×10^5) were cotransfected with C/EBP reporter (100 ng) and the indicated plasmids (C, empty vector of NLK; N, NLK-expressing plasmids; FL, full-length ATF5). Twenty-four hours after transfection, reporter assays were performed. (E) Effects of adding C- or N-terminal EGFP to ATF5 on NLK-cooperating C/EBP activation. The experiment was performed as for panel D, and the fold changes are indicated. The graphs present means and SD. The asterisks indicate a significant difference ($P < 0.05$) calculated by one-way analysis of variance followed by Tukey's multiple-comparison test.

report that ATF5 interacts with C/EBPβ and enhances its transactivation of C/EBPα (27), our results also supported the notion that ATF5 activates C/EBP. Moreover, NLK cooperated with ATF5 to activate C/EBP, and ATF5 was dispensable for the activation of C/EBP by NLK. IL-1β-induced C/EBP activation was significantly weakened when NLK was knocked out. These results suggest that NLK is involved in basal and IL-1β-stimulated C/EBP activation in an ATF5-dependent fashion.

Recently, it has been demonstrated that the N-terminal amino acids of ATF5 are important for IL-1β-induced ATF5 stabilization, which is mainly controlled by proteasome-mediated proteolysis (31). Similarly, in our experiments, we found that the N-terminal residues of ATF5 conferred NLK-induced stabilization, which was significantly blocked by proteasome inhibition. Furthermore, both IL-1β-induced ATF5 stabilization and C/EBP activation were blunted by NLK knockdown or knockout. These results suggest that NLK stabilizes ATF5 to potentiate basal and IL-1β-triggered C/EBP activation. Future studies should explore the physiological function, especially *in vivo*, and the underlying mechanism of basal and IL-1β-regulated ATF5 stabilization by NLK.

It should be noted that NLK also phosphorylated ATF5; however, this event was not responsible for ATF5 stabilization by NLK. Several ATF/CREB family members, such as ATF2, require the phosphorylation of Ser/Thr residues in the transactivation domain to activate their capacities for transactivation. However, ATF5 contains a constitutively active transcriptional activation domain that does not appear to require phosphorylation (47), which was supported by our observation that ATF5-6A activated C/EBP as efficiently as wild-type ATF5. We also observed that NLK did not alter the localization of ATF5 and that the localization of ATF5-6A was similar to that of wild-type ATF5. Therefore, NLK may play a dual role in modulating ATF5. Stabilization of ATF5 by NLK may globally enhance its functions, including activation of C/EBP; however, phosphorylation of ATF5 by NLK may selectively control ATF5 through an as-yet unknown mechanism (e.g., by affecting its interaction with its binding partners or affecting other ATF5 modifications). Further studies are necessary to explore the basic and physiological functions of NLK-induced phosphorylation of ATF5.

C/EBP and ATF5 transcription factors play critical roles in a broad range of physiological and pathological processes, including immunity, inflammation, cell proliferation, and differentiation. IL-1β is a proinflammatory cytokine that initiates several signaling cascades, including that involving C/EBP. Thus, our

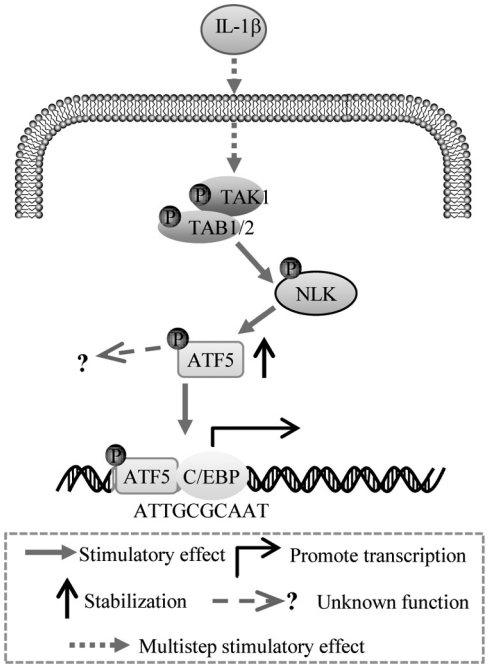

FIG 9 Schematic model for the involvement of TAK1-NLK in IL-1β-triggered ATF5 stabilization and C/EBP activation.

finding that TAK1-NLK positively regulated IL-1β-stimulated C/EBP activation by inhibiting proteasome-mediated proteolysis of ATF5 (Fig. 9) may provide a future therapeutic target for disease control.

ACKNOWLEDGMENTS

We thank Yan Zhou, Zan Huang, and Ying-Wen Ding for stimulating discussions.

This work was supported by grants from the National Basic Research Program of China (2011CB944404), the National Natural Science Foundation of China (81270306), the National Science and Technology Support Project (2012BAI39B02, 2012BAI39B03, and 2014BAI02B01), the Trans-Century Training Programme Foundation for the Talents by the State Education Commission (NCET-10-0655), and Fundamental Research Funds for the Central Universities (204275771).

REFERENCES

1. **Kojima H, Sasaki T, Ishitani T, Iemura S, Zhao H, Kaneko S, Kunimoto H, Natsume T, Matsumoto K, Nakajima K.** 2005. STAT3 regulates Nemo-like kinase by mediating its interaction with IL-6-stimulated TGFbeta-activated kinase 1 for STAT3 Ser-727 phosphorylation. Proc Natl Acad Sci U S A **102:** 4524–4529. http://dx.doi.org/10.1073/pnas.0500679102.
2. **Smit L, Baas A, Kuipers J, Korswagen H, van de Wetering M, Clevers H.** 2004. Wnt activates the Tak1/Nemo-like kinase pathway. J Biol Chem **279:**17232–17240. http://dx.doi.org/10.1074/jbc.M307801200.
3. **Ohkawara B, Shirakabe K, Hyodo-Miura J, Matsuo R, Ueno N, Matsumoto K, Shibuya H.** 2004. Role of the TAK1-NLK-STAT3 pathway in TGF-beta-mediated mesoderm induction. Genes Dev **18:**381–386. http://dx.doi.org/10.1101/gad.1166904.
4. **Kanei-Ishii C, Ninomiya-Tsuji J, Tanikawa J, Nomura T, Ishitani T, Kishida S, Kokura K, Kurahashi T, Ichikawa-Iwata E, Kim Y, Matsumoto K, Ishii S.** 2004. Wnt-1 signal induces phosphorylation and degradation of c-Myb protein via TAK1, HIPK2, and NLK. Genes Dev **18:**816–829. http://dx.doi.org/10.1101/gad.1170604.
5. **Ishitani T, Kishida S, Hyodo-Miura J, Ueno N, Yasuda J, Waterman M, Shibuya H, Moon RT, Ninomiya-Tsuji J, Matsumoto K.** 2003. The TAK1-NLK mitogen-activated protein kinase cascade functions in the Wnt-5a/Ca(2+) pathway to antagonize Wnt/beta-catenin signaling. Mol Cell Biol **23:**131–139. http://dx.doi.org/10.1128/MCB.23.1.131-139.2003.
6. **Meneghini MD, Ishitani T, Carter JC, Hisamoto N, Ninomiya-Tsuji J, Thorpe CJ, Hamill DR, Matsumoto K, Bowerman B.** 1999. MAP kinase and Wnt pathways converge to downregulate an HMG-domain repressor in Caenorhabditis elegans. Nature **399:**793–797. http://dx.doi.org/10.1038/21666.
7. **Zhang HH, Li SZ, Zhang ZY, Hu XM, Hou PN, Gao L, Du RL, Zhang XD.** 2014. Nemo-like kinase is critical for p53 stabilization and function in response to DNA damage. Cell Death Differ **21:**1656–1663. http://dx.doi.org/10.1038/cdd.2014.78.
8. **Li SZ, Zhang HH, Liang JB, Song Y, Jin BX, Xing NN, Fan GC, Du RL, Zhang XD.** 2014. Nemo-like kinase (NLK) negatively regulates NF-kappa B activity through disrupting the interaction of TAK1 with IKKbeta. Biochim Biophys Acta **1843:**1365–1372. http://dx.doi.org/10.1016/j.bbamcr.2014.03.028.
9. **Freeman M, Bienz M.** 2001. EGF receptor/Rolled MAP kinase signalling protects cells against activated Armadillo in the Drosophila eye. EMBO Rep **2:**157–162. http://dx.doi.org/10.1093/embo-reports/kve019.
10. **Rocheleau CE, Yasuda J, Shin TH, Lin R, Sawa H, Okano H, Priess JR, Davis RJ, Mello CC.** 1999. WRM-1 activates the LIT-1 protein kinase to transduce anterior/posterior polarity signals in C. elegans. Cell **97:**717–726. http://dx.doi.org/10.1016/S0092-8674(00)80784-9.
11. **Kortenjann M, Nehls M, Smith AJ, Carsetti R, Schuler J, Kohler G, Boehm T.** 2001. Abnormal bone marrow stroma in mice deficient for Nemo-like kinase, Nlk. Eur J Immunol **31:**3580–3587. http://dx.doi.org/10.1002/1521-4141(200112)31:12<3580::AID-IMMU3580>3.0.CO;2-N.
12. **Tsukada J, Yoshida Y, Kominato Y, Auron PE.** 2011. The CCAAT/enhancer (C/EBP) family of basic-leucine zipper (bZIP) transcription factors is a multifaceted highly-regulated system for gene regulation. Cytokine **54:**6–19. http://dx.doi.org/10.1016/j.cyto.2010.12.019.
13. **Poli V.** 1998. The role of C/EBP isoforms in the control of inflammatory and native immunity functions. J Biol Chem **273:**29279–29282. http://dx.doi.org/10.1074/jbc.273.45.29279.
14. **Lekstrom-Himes J, Xanthopoulos KG.** 1998. Biological role of the CCAAT/enhancer-binding protein family of transcription factors. J Biol Chem **273:**28545–28548. http://dx.doi.org/10.1074/jbc.273.44.28545.
15. **Nerlov C.** 2008. C/EBPs: recipients of extracellular signals through proteome modulation. Curr Opin Cell Biol **20:**180–185. http://dx.doi.org/10.1016/j.ceb.2008.02.002.
16. **Hungness ES, Pritts TA, Luo GJ, Hershko DD, Robb BW, Hasselgren PO.** 2002. IL-1beta activates C/EBP-beta and delta in human enterocytes through a mitogen-activated protein kinase signaling pathway. Int J Biochem Cell Biol **34:**382–395. http://dx.doi.org/10.1016/S1357-2725(01)00129-7.
17. **Magalini A, Savoldi G, Ferrari F, Garnier M, Ghezzi P, Albertini A, Di Lorenzo D.** 1995. Role of IL-1 beta and corticosteroids in the regulation of the C/EBP-alpha, beta and delta genes in vivo. Cytokine **7:**753–758. http://dx.doi.org/10.1006/cyto.1995.0090.
18. **Svotelis A, Doyon G, Bernatchez G, Desilets A, Rivard N, Asselin C.** 2005. IL-1 beta-dependent regulation of C/EBP delta transcriptional activity. Biochem Biophys Res Commun **328:**461–470. http://dx.doi.org/10.1016/j.bbrc.2005.01.002.
19. **Yan C, Wang X, Cao J, Wu M, Gao H.** 2012. CCAAT/enhancer-binding protein gamma is a critical regulator of IL-1beta-induced IL-6 production in alveolar epithelial cells. PLoS One **7:**e35492. http://dx.doi.org/10.1371/journal.pone.0035492.
20. **Yang Z, Zhu X, Guo C, Sun K.** 2009. Stimulation of 11beta-HSD1 expression by IL-1beta via a C/EBP binding site in human fetal lung fibroblasts. Endocrine **36:**404–411. http://dx.doi.org/10.1007/s12020-009-9245-4.
21. **Fields J, Ghorpade A.** 2012. C/EBPbeta regulates multiple IL-1beta-induced human astrocyte inflammatory genes. J Neuroinflammation **9:**177. http://dx.doi.org/10.1186/1742-2094-9-177.
22. **Acuner Ozbabacan SE, Gursoy A, Nussinov R, Keskin O.** 2014. The structural pathway of interleukin 1 (IL-1) initiated signaling reveals mechanisms of oncogenic mutations and SNPs in inflammation and cancer. PLoS Comput Biol **10:**e1003470. http://dx.doi.org/10.1371/journal.pcbi.1003470.
23. **Weber A, Wasiliew P, Kracht M.** 2010. Interleukin-1 (IL-1) pathway. Sci Signal **3:**cm1. http://dx.doi.org/10.1126/scisignal.3105cm1.
24. **Chen ZJ.** 2005. Ubiquitin signalling in the NF-kappaB pathway. Nat Cell Biol **7:**758–765. http://dx.doi.org/10.1038/ncb0805-758.
25. **Greene LA, Lee HY, Angelastro JM.** 2009. The transcription factor ATF5:

role in neurodevelopment and neural tumors. J Neurochem **108:**11–22. http://dx.doi.org/10.1111/j.1471-4159.2008.05749.x.
26. **Newman JR, Keating AE.** 2003. Comprehensive identification of human bZIP interactions with coiled-coil arrays. Science **300:**2097–2101. http://dx.doi.org/10.1126/science.1084648.
27. **Zhao Y, Zhang YD, Zhang YY, Qian SW, Zhang ZC, Li SF, Guo L, Liu Y, Wen B, Lei QY, Tang QQ, Li X.** 2014. p300-dependent acetylation of ATF5 enhances C/EBPbeta transactivation of C/EBPalpha during 3T3-L1 differentiation. Mol Cell Biol **34:**315–324. http://dx.doi.org/10.1128/MCB.00956-13.
28. **Wei Y, Jiang J, Liu D, Zhou J, Chen X, Zhang S, Zong H, Yun X, Gu J.** 2008. Cdc34-mediated degradation of ATF5 is blocked by cisplatin. J Biol Chem **283:**18773–18781. http://dx.doi.org/10.1074/jbc.M707879200.
29. **Watatani Y, Kimura N, Shimizu YI, Akiyama I, Tonaki D, Hirose H, Takahashi S, Takahashi Y.** 2007. Amino acid limitation induces expression of ATF5 mRNA at the post-transcriptional level. Life Sci **80:**879–885. http://dx.doi.org/10.1016/j.lfs.2006.11.013.
30. **Uekusa H, Namimatsu M, Hiwatashi Y, Akimoto T, Nishida T, Takahashi S, Takahashi Y.** 2009. Cadmium interferes with the degradation of ATF5 via a post-ubiquitination step of the proteasome degradation pathway. Biochem Biophys Res Commun **380:**673–678. http://dx.doi.org/10.1016/j.bbrc.2009.01.158.
31. **Abe T, Kojima M, Akanuma S, Iwashita H, Yamazaki T, Okuyama R, Ichikawa K, Umemura M, Nakano H, Takahashi S, Takahashi Y.** 2014. N-terminal hydrophobic amino acids of ATF5 confer IL-1beta-induced stabilization. J Biol Chem **289:**3888–3900. http://dx.doi.org/10.1074/jbc.M113.491217.
32. **Zhang X, Guo C, Chen Y, Shulha HP, Schnetz MP, LaFramboise T, Bartels CF, Markowitz S, Weng Z, Scacheri PC, Wang Z.** 2008. Epitope tagging of endogenous proteins for genome-wide ChIP-chip studies. Nat Methods **5:**163–165. http://dx.doi.org/10.1038/nmeth1170.
33. **Huang P, Xiao A, Zhou M, Zhu Z, Lin S, Zhang B.** 2011. Heritable gene targeting in zebrafish using customized TALENs. Nat Biotechnol **29:**699–700. http://dx.doi.org/10.1038/nbt.1939.
34. **Ran FA, Hsu PD, Wright J, Agarwala V, Scott DA, Zhang F.** 2013. Genome engineering using the CRISPR-Cas9 system. Nat Protoc **8:**2281–2308. http://dx.doi.org/10.1038/nprot.2013.143.
35. **Hu B, Li S, Zhang X, Zheng X.** 2014. HSCARG, a novel regulator of H2A ubiquitination by downregulating PRC1 ubiquitin E3 ligase activity, is essential for cell proliferation. Nucleic Acids Res **42:**5582–5593. http://dx.doi.org/10.1093/nar/gku230.
36. **Vallejo M, Ron D, Miller CP, Habener JF.** 1993. C/ATF, a member of the activating transcription factor family of DNA-binding proteins, dimerizes with CAAT/enhancer-binding proteins and directs their binding to cAMP response elements. Proc Natl Acad Sci U S A **90:**4679–4683. http://dx.doi.org/10.1073/pnas.90.10.4679.
37. **Ishitani T, Ishitani S.** 2013. Nemo-like kinase, a multifaceted cell signaling regulator. Cell Signal **25:**190–197. http://dx.doi.org/10.1016/j.cellsig.2012.09.017.
38. **Kinoshita E, Kinoshita-Kikuta E, Takiyama K, Koike T.** 2006. Phosphate-binding tag, a new tool to visualize phosphorylated proteins. Mol Cell Proteomics **5:**749–757. http://dx.doi.org/10.1074/mcp.T500024-MCP200.
39. **Xue Y, Ren J, Gao X, Jin C, Wen L, Yao X.** 2008. GPS 2.0, a tool to predict kinase-specific phosphorylation sites in hierarchy. Mol Cell Proteomics **7:**1598–1608. http://dx.doi.org/10.1074/mcp.M700574-MCP200.
40. **Obenauer JC, Cantley LC, Yaffe MB.** 2003. Scansite 2.0: proteome-wide prediction of cell signaling interactions using short sequence motifs. Nucleic Acids Res **31:**3635–3641. http://dx.doi.org/10.1093/nar/gkg584.
41. **Ciechanover A.** 2005. Proteolysis: from the lysosome to ubiquitin and the proteasome. Nat Rev Mol Cell Biol **6:**79–87. http://dx.doi.org/10.1038/nrm1552.
42. **Kim S, Kim Y, Lee J, Chung J.** 2010. Regulation of FOXO1 by TAK1-Nemo-like kinase pathway. J Biol Chem **285:**8122–8129. http://dx.doi.org/10.1074/jbc.M110.101824.
43. **Ishitani T, Ninomiya-Tsuji J, Nagai S, Nishita M, Meneghini M, Barker N, Waterman M, Bowerman B, Clevers H, Shibuya H, Matsumoto K.** 1999. The TAK1-NLK-MAPK-related pathway antagonizes signalling between beta-catenin and transcription factor TCF. Nature **399:**798–802. http://dx.doi.org/10.1038/21674.
44. **Jiang Z, Ninomiya-Tsuji J, Qian Y, Matsumoto K, Li X.** 2002. Interleukin-1 (IL-1) receptor-associated kinase-dependent IL-1-induced signaling complexes phosphorylate TAK1 and TAB2 at the plasma membrane and activate TAK1 in the cytosol. Mol Cell Biol **22:**7158–7167. http://dx.doi.org/10.1128/MCB.22.20.7158-7167.2002.
45. **Strippoli R, Benedicto I, Perez Lozano ML, Pellinen T, Sandoval P, Lopez-Cabrera M, del Pozo MA.** 2012. Inhibition of transforming growth factor-activated kinase 1 (TAK1) blocks and reverses epithelial to mesenchymal transition of mesothelial cells. PLoS One **7:**e31492. http://dx.doi.org/10.1371/journal.pone.0031492.
46. **Takaesu G, Ninomiya-Tsuji J, Kishida S, Li X, Stark GR, Matsumoto K.** 2001. Interleukin-1 (IL-1) receptor-associated kinase leads to activation of TAK1 by inducing TAB2 translocation in the IL-1 signaling pathway. Mol Cell Biol **21:**2475–2484. http://dx.doi.org/10.1128/MCB.21.7.2475-2484.2001.
47. **Al Sarraj J, Vinson C, Thiel G.** 2005. Regulation of asparagine synthetase gene transcription by the basic region leucine zipper transcription factors ATF5 and CHOP. Biol Chem **386:**873–879. http://dx.doi.org/10.1515/BC.2005.102.